Journal of Materials Chemistry A

PAPER

View Article Online
View Journal | View Issue

Cite this: J. Mater. Chem. A, 2015, 3, 16190

# Fast magnetically driven electrodeposition of amorphous metal oxide water oxidation catalysts from carbon-coated metallic nanoparticles†

Jing Zhu,[ac] François Lambert,[a] Clotilde Policar,[a] François Mavré*[b] and Benoît Limoges*[b]

Received 10th May 2015
Accepted 26th June 2015

DOI: 10.1039/c5ta03430b

www.rsc.org/MaterialsA

We report a new approach for efficient electrodeposition of amorphous metal oxide water oxidation catalysts on an electrode surface. A catalytic metal-based film was obtained by means of anodic oxidation of metallic nanoparticles, namely carbon-coated cobalt nanoparticles or carbon-coated nickel nanoparticles. Interestingly, these particles are intrinsically conductive and possess magnetic properties which make it easy to collect them on an electrode surface using a simple magnet to form a porous conductive particulate film. Upon anodic polarization in an appropriate electrolyte, the particulate film is rapidly converted into an amorphous metal-based catalytic film that efficiently catalyzes the oxidation of water at neutral pH. Compared to Nocera's method based on anodic electrodeposition of a metal salt in solution, this new electrodeposition strategy offers the key advantage of supplying metal ions in a solid and metallic form, leading to a fast release of high local concentrations of metal ions right at the spot of the film formation (*i.e.*, in the vicinity of the electrode surface). This plays a decisive role in the formation rate of the catalytic film, allowing the deposition of the oxygen-evolving catalyst in a remarkably short-time. Moreover, the methodology can be easily extended to a wide range of metal particles of different nature and sizes, and also to their mixtures, finally offering a new degree of flexibility and opportunities not only in the preparation of metal-based water oxidation catalysts, but also in the preparation of inorganic metal-based catalysts for hydrogen or oxygen evolution.

## Introduction

Oxidation of water into $O_2$ is a critical step in water splitting, a process that would be a key technology component of a hydrogen economy.[1–3] However, the development of manufacturable large-scale water electrolyzers or photoelectrolyzers under chemically benign conditions and using renewable energies still remains a major scientific and technological challenge.[2,4] This is in part due to the fact that water oxidation at standard electrodes (or oxygen evolution reaction, OER) requires a large excess energy in the form of an overpotential to overcome the activation barriers resulting from the four-electron oxidation of two water molecules coupled to the removal of four protons to form an oxygen–oxygen bond. Water oxidation catalysts (WOCs) based on noble metals or metal oxides like $IrO_2$ or $RuO_2$ have been shown to be effective anode electrocatalysts to lower the OER overpotential.[1] However, technologies based on these expensive catalysts are not competitive in the development of nonconcentrated solar energy storage applications. Moreover, they need to operate under harsh physical and chemical conditions, which is a further impediment to large-scale development. Therefore, finding inexpensive water oxidation materials that can be both easily manufactured at low-cost and can operate under simple conditions is a key step toward the viability of the concept of personalized energy storage *via* water splitting.[5]

Among the different earth-abundant and low-cost WOCs so far reported, many are based on crystalline transition metal oxides, in particular metal oxides of Fe, Ni, Co and Mn, or their alloys.[1,6] An important advantage of these metal-based inorganic catalysts is their relatively high stability under harsh and extreme oxidative conditions required for the OER.[7] However, their oxygen-evolving catalytic activities are essentially high in concentrated basic solutions (pH > 13) but rather low in neutral water. It is only recently that earth-abundant and easily manufacturable amorphous metal oxide-based oxygen-evolving catalysts have been discovered to operate efficiently in neutral water and under ambient conditions.[8,9] This was first demonstrated

[a]*École Normale Supérieure – PSL Research University, Département de Chimie, Sorbonne Universités – UPMC Univ Paris 06, CNRS UMR 7203 LBM, 24 rue Lhomond, F-75005 Paris, France*

[b]*Laboratoire d'Electrochimie Moléculaire, UMR 7591 CNRS, Université Paris Diderot, Sorbonne Paris Cité, 15 rue Jean-Antoine de Baïf, F-75205 Paris Cedex 13, France. E-mail: limoges@univ-paris-diderot.fr; Fax: +33 157278788; Tel: +33 157278789*

[c]*East China Normal University, Department of Chemistry, 500 Dongchuan Road, Shanghai 200241, China*

† Electronic supplementary information (ESI) available: Experimental section and Fig. S1–S9. See DOI: 10.1039/c5ta03430b

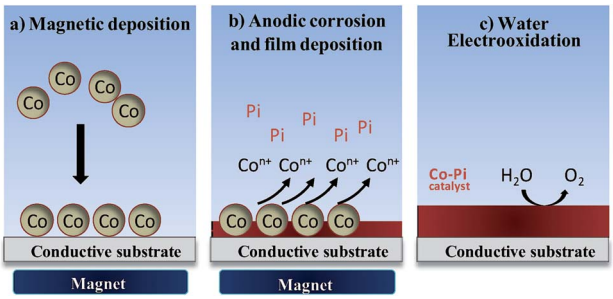


Scheme 1 Sequential steps of catalyst electrodeposition, illustrated here in the case of magnetic cobalt nanoparticles.

by Nocera and collaborators by electrodeposition of a catalytically active amorphous cobalt oxide/hydroxide film on an inert electrode from simple anodic electrode polarization in a neutral phosphate solution of $Co^{2+}$.[8] Similar electrodeposition strategies were afterward reported for the preparation of amorphous catalytic films of Ni-, Fe-, and Mn-based metal oxides in neutral or slightly basic aqueous solutions.[9–12] Alternatively, it was shown that amorphous Co- and Ni-based WOCs can be generated by anodic processing of a bulk metallic film either sputtered[13] or electron beam vaporized on a solid substrate,[14] or through a photochemical route involving the photodegradation of transition metal complexes.[15,16]

Here, we describe a new strategy to generate an inorganic amorphous catalytic metal oxide film on an electrode surface by means of anodic oxidation of metallic nanoparticles, in particular carbon-coated cobalt (or nickel) nanoparticles. Interestingly, these particles are intrinsically conductive and possess magnetic properties which make it easy to collect and assemble on a flat electrode surface by means of a simple magnet to form a particulate conductive film (Scheme 1). The resulting porous network of nanoparticles can then be anodically corroded in an appropriately buffered environment so as to generate a catalytically active film for water oxidation at neutral pH.

## Results and discussion

The magnetic carbon-coated metal nanoparticles we investigated are all commercially available. We first focused on carbon-coated cobalt particles (C/Co-NPs). The commercial nanoparticles are provided as a powder with particle size <100 nm and an average size of ~25 nm (Fig. S1 in ESI†). XRD analysis showed a pure cobalt cubic phase (Fig. S2†). These metal-based nanoparticles have the peculiarities to be air- and thermally stable, electrically conductive (resistivity of 6.24 μΩ $cm^{-1}$ at 20 °C) and also magnetic (>150 emu $g^{-1}$).[17] They are surrounded by a chemically inert graphitized carbon shell (with a total carbon content <8%) that is assumed to protect the metallic core from air oxidation.[17] The core–shell arrangement is obtained by adding acetylene during the reducing flame spray synthesis of the nanoparticles, thus resulting in controlled deposition of a multilayer graphene-coating on the particle surface. According to their excellent magnetic properties, they can also be easily manipulated and collected under the action of a magnetic field.[17]

For electrochemical experiments, the magnetic powder has been first dispersed in water (from 0.5 to 50 mg $mL^{-1}$) in the presence of a surfactant (0.1 wt% Tween 20), leading to a homogenous suspension after 5 min ultrasonication. The colloidal suspension was then half-to-half mixed with a sodium phosphate (NaPi) buffer solution (0.2 M, pH 7.0) and a droplet of 40 μL was then deposited on the surface of a flat ITO electrode delimited by an insulating eyelet (that defines a small circular electrochemical cell with a working disk ITO area of ~0.2 $cm^2$). ITO was chosen for its transparency, facilitating the naked-eye observation of the particle deposition. Using a cylindrical magnet (whose diameter is similar to that of the working ITO disk electrode) positioned underneath the electrode, the magnetic particles were rapidly collected at the working electrode/solution interface. Depending on the amount of particles initially present in the droplet (*i.e.*, ranging from 0.01 to 1 mg in the 40 μL), nanoporous particulate films with thicknesses ranging from a few tens of nanometers (*i.e.*, corresponding to the thickness of a single layer of particles) to several micrometers were obtained (which corresponds to a weight particles per unit area ranging from 0.05 to 5 mg $cm^{-2}$).

Cyclic voltammetry (CV) of an almost single layer of C/Co-NPs on ITO (*i.e.*, 0.05 mg $cm^{-2}$) exhibits a strong irreversible anodic wave in a 0.1 M NaPi buffer (pH 7.0) that onsets at ~1.2 V (*vs.* NHE) and then rapidly increases up to a current density >10 mA $cm^{-2}$ at 1.6 V (curve a in Fig. 1), while at a bare ITO electrode in the same buffer, there is no discernible response except the background charging current (curve e in Fig. 1). On subsequent scans, the irreversible oxidation wave is observed rather stable except for the small anodic prefeature at the foot of the oxidation wave and the small cathodic wave on the reverse scan which both tend to slowly grow upon repetitive scanning, suggesting the adsorption/deposition of an electroactive species. Since there is no other electron donor than water in solution, it is hypothesized that this strong irreversible anodic response arises from a catalytic oxidation of water by the particulate film. To disclose the origin of this catalytic activity, immediately after the C/Co-NP-coated ITO was scanned by CV, the electrode was removed from the magnet support, thoroughly rinsed with water (so as to withdraw all nanoparticles that are not retained on the surface, *vide infra*), and then placed in a fresh 0.1 M NaPi buffer. The subsequent CV of the rinsed electrode still shows a strong irreversible anodic current (curve a′ in Fig. 1) indicative of the deposit of a catalytically active film on the electrode surface. To confirm that this deposit effectively arises from the anodic polarization of the particulate film, the experiment was repeated with a new C/Co-NP-coated ITO electrode that was scanned only once by CV in a potential window far below the onset of the catalytic wave (*i.e.* at $E < 0.9$ V) and next examined by CV in a fresh electrolyte solution. The resultant CV was identical to the background charging current recorded at a bare ITO electrode (data not shown) demonstrating that the active film is generated only after the particulate film is polarized at a sufficiently anodic potential. It also suggests that the magnetic

particles act as a precursor to the anodic electrodeposition of a water oxidation catalytic film.

Comparison of the CV obtained with the C/Co-NPs on ITO (curve a in Fig. 1) to the CV of a solution of $Co(NO_3)_2$ (0.5 mM) in 0.1 M NaPi (curves c in Fig. 1) points out some similarities but also differences. Both catalytic waves display a small anodic prewave (~1.2 V) at the foot of the strong catalytic oxidation wave (curves a and c in the right bottom of Fig. 1). This prewave was previously assigned by Nocera and collaborators[18] to the oxidation of $Co^{2+}$ in $Co^{3+}$ species,[19] which in the presence of a coordinating and proton-accepting anion in the electrolyte (*i.e.* phosphate anion) leads to the deposition of a thin amorphous cobalt-based catalytic film on the electrode surface (according to a nucleation and growth process[20]). Even though there is a difference in the starting state of cobalt in the two systems, it is most likely that a similar electrochemical deposition process occurs here too with the C/Co-NPs on ITO. A closer inspection of the CVs recorded with the particulate film shows, from an onset potential of −0.25 V, the presence of a very weak and broad anodic response preceding the small anodic prewave (see the zoom of curve a in the left top inset of Fig. 1), a behavior that is not observed on the CV of a $Co^{2+}$ solution. Besides, the latter weak and broad response disappears once the particles are washed out from the electrode surface (curve a′ in the left top inset of Fig. 1), while the anodic prewave at the foot of the catalytic wave remains and is even augmented (curve a′ in Fig. 1). On account of the onset potential at which the weak anodic current starts to increase (*i.e.*, ~−0.25 V, which is close to the standard reduction potential of the $Co^{2+}/Co^0$ couple, *i.e.* $E^0_{Co^{2+}/Co} = -0.28$ V at pH 0 (ref. 21)) and also of the presence of the anodic prewave at 1.2 V assigned to the oxidation of $Co^{II}$ ions in solution, we have concluded that the weak and broad anodic current corresponds to the direct electrochemical oxidation of the cobalt metal ($Co^0$) contained in the nanoparticles into $Co^{II}$ ions. On the basis of this finding, one could thus state that under anodic electrode polarization, the C/Co-NPs electrically wired to the ITO surface are anodically corroded with dissolution of $Co^{II}$, thus leading to the release of high local concentrations of soluble $Co^{II}$ (or $Co^{III}$ at higher anodic potential) in the vicinity of the particulate film (a behavior that was initially unexpected because of the known resistance of C/Co-NPs to air-oxidation). Consequently, in the presence of a proton-accepting electrolyte and the application of a sufficiently anodic potential to generate $Co^{III}$, the conditions are locally gathered to efficiently form an amorphous cobalt oxide/hydroxide film (*i.e.*, a CoPi film), similar to that previously reported by Nocera and collaborators.[8,18]

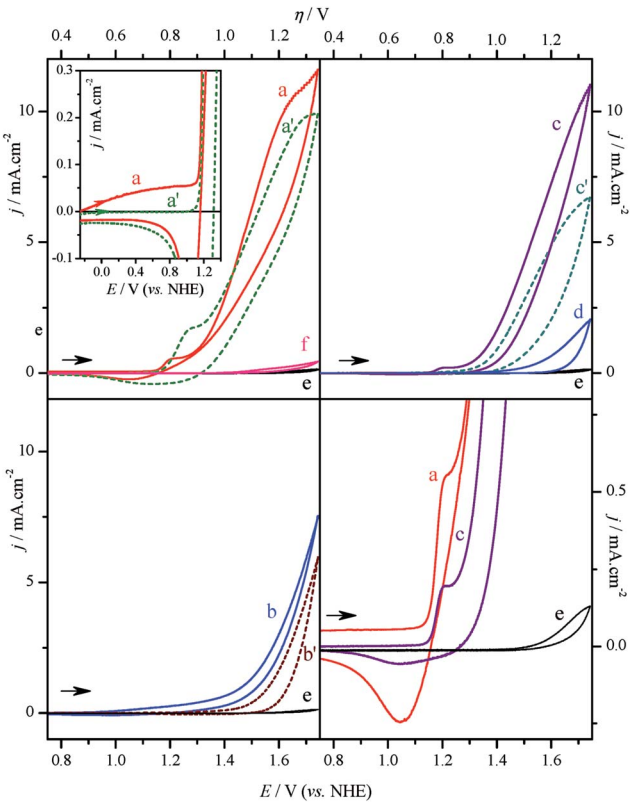


Fig. 1 Left top: (a) First CV scans recorded at C/Co-NP-coated ITO electrodes (0.05 mg $cm^{-2}$) in 0.1 M NaPi (pH 7.0) and (a′) second CV scans recorded after the same electrode was thoroughly washed with water and then placed in the same fresh electrolyte. (e) CV blank response at a bare ITO electrode in 0.1 M NaPi. (f) CV at the $Co_3O_4$ nanoparticle-coated ITO electrode in 0.1 M NaPi. Inset: zoom of the CVs (a) and (a′) in the lower potential range. Left bottom: (b) First CV scans recorded at C/Co-NP-coated ITO electrodes (0.05 mg $cm^{-2}$) in 0.1 M $Na_2SO_4$ and (b′) second CV scans recorded after the same electrode was thoroughly washed with water and then placed in the same fresh electrolyte. Right top: (c and d) First CVs recorded at ITO electrodes in 0.5 mM $Co(NO_3)_2$ solution prepared in (c) 0.1 M NaPi or (d) 0.1 M $Na_2SO_4$, and (c′) second CV (cyan) recorded after the electrode in (c) was thoroughly washed with water and then placed in the same fresh electrolyte than during the first scan, *i.e.* 0.1 M NaPi. Right bottom: Zoom of the CVs (a), (c) and (e) in the prewave potential range. The top scale represents the overpotential $\eta(j) = E(j) - (E^0_{O_2/H_2O} - 0.059 \times \text{pH})$. All CVs were performed at room temperature and at a scan rate $v = 0.1$ V $s^{-1}$.

The fact that an amorphous film of CoPi forms over the electrode surface is supported by the strong dependence of the film formation on the nature of the proton-accepting electrolyte. This is illustrated by the CV curve b in Fig. 1 which shows for a C/Co-NP-coated ITO in a poor proton-accepting electrolyte (*i.e.*, 0.1 M $Na_2SO_4$, pH ~ 6.5) a strong shift of the catalytic wave to high overpotentials along with a disappearance of the small anodic wave related to the oxidation of $Co^{II}$ to $Co^{III}$. Furthermore, after removing nanoparticles from the electrode surface by rinsing, a further anodic shift of the catalytic wave is observed (curve b′ in Fig. 1), suggesting a poor stability of the Co-based film that may form under these conditions. These results are in line with that previously found with the electrodeposition of a CoPi film from a solution of $Co^{2+}$ and for which the film formation was strongly impede when performed in a poor proton-accepting electrolyte (see curve d in Fig. 1).[18] Moreover, by analogy with the CoPi catalyst, it is anticipated that the phosphate coordinating anion helps to stabilize the deposited amorphous film through a self-healing process.[8]

Another interesting observation that can be inferred from direct comparison of the CVs obtained at the C/Co-NP-coated electrode and at the bare ITO electrode in a solution of $Co^{2+}$ (comparison of curves a and c in Fig. 1, right bottom graph) is a

 

significant shift of the onset catalytic wave to lower overpotentials, clearly suggesting a faster film formation and/or higher activation from a cobalt particulate film than from a $Co^{2+}$ solution. This can be explained by the fact that the concentration of $Co^{2+}$ locally released (*i.e.* in the vicinity of the electrode surface) by corrosion of the C/Co-NPs is far greater than that reached by simple solubilisation of a cobalt nitrate salt in a 0.1 M phosphate buffer (at room temperature, the limit of solubility of cobalt nitrate in this buffer is below 1 mM). This is also supported by the fact that a quite high concentration of EDTA (30 mM) was required to fully inhibit the amorphous catalytic film formation from the cobalt-based particulate film (*i.e.*, by scavenging the released $Co^{2+}$), while when starting from a 0.5 mM solution of cobalt nitrate, a stoichiometric concentration of EDTA was sufficient to stop the anodic electrodeposition of the catalytic film (Fig. S3†). Given the first order rate in the cobalt concentration previously determined for the electrochemical growth of a CoPi film,[20] the local release of much higher amounts of $Co^{II}$ ions from anodic corrosion of cobalt-based particulate films would definitely accelerate the film formation. The comparatively higher activity of our deposited film is therefore assumed to be mainly related to a faster film formation of cobalt-based WOC than a change in the nature of the catalyst itself.

To complete the study, a particulate film of $Co_3O_4$ nanoparticles (commercial nanopowder with an average size < 50 nm) on ITO was also examined (these particles being not magnetic, the particulate film was obtained by drop-casting). Since the cobalt atoms of these nanoparticles are already in a stable oxidized form, one can anticipate that unlike C/Co-NPs, they cannot be electrochemically corroded to form a cobalt-based catalytic film. This is effectively what we can infer from curve f in Fig. 1, where the CV of a $Co_3O_4$ particulate film in a 0.1 M NaPi does not show any significant anodic wave. This result highlights the poor WOC properties of $Co_3O_4$ at neutral pH, a behavior that is in striking contrast to the high activities observed for the C/Co-NPs, but also in contrast to the catalytic activities previously reported for analogous $Co_3O_4$ nanoparticles[6] either in strongly basic aqueous solutions[22–25] or in slightly acidic solutions.[26,27]

With the aim to assess the production of $O_2$ by the catalyst, but also to evaluate the faradic efficiency of the catalytic oxidation reaction, an experiment at a rotating ring-disk electrode (RRDE) was carried out in a standard three-electrode electrochemical cell (Fig. 2). The central glassy carbon (GC) disk was first coated by a catalytic film from anodic polarization of a particulate film of C/Co-NPs (0.1 mg $cm^{-2}$) at a controlled potential (*i.e.*, at 1.24 V for 10 min) in 0.1 M NaPi. After electrode rinsing and immersion in a 1 M NaOH, the central glassy carbon (GC) disk was then subjected to a linear scan from 0 to 1.0 V at a constant rotation rate of 1600 rpm under 1 atm $N_2$, while the potential at the Pt ring electrode was held at −0.46 V to rapidly reduce $O_2$ to $H_2O_2$.[28] The resulting *j*–*E* plot is shown in Fig. 2. While the catalytic anodic current at the disk electrode was increased, the cathodic current at the ring proportionally increased. This clearly shows that dioxygen is produced at the catalytic film. The faradaic efficiency ($\varepsilon$) of the OER catalyst is proportional to the ratio of the ring current ($i_r$) to the disk current ($i_d$) and inversely proportional to the collection efficiency $N$ of the RRDE (*i.e.* with our RRDE, $N = 0.37$) according to the following relationship: $\varepsilon = 2i_r/i_dN$. A faradaic efficiency $\varepsilon \geq 0.9$ was found (determined at 1 mA $cm^{-2}$) which is in line with that generally found for efficient heterogeneous WOCs.[7] It is worth noting that under strong alkaline conditions (1 M NaOH, pH 14) and for the particular film we have used (*i.e.*, 10 min electrodeposition at a constant potential of 1.24 V), an overpotential for water oxidation of only 510 mV (uncorrected for cell resistance)/390 mV (corrected for 60 Ω cell resistance) is obtained at a current density of 10 mA $cm^{-2}$ (see the horizontal dashed line in Fig. 2 which corresponds to the current density expected for a 10% efficient solar water-splitting device[29]). This value is similar to those reported for CoPi-based WOCs in alkaline solution.[7] From graphical representation of the log of catalytic current density *versus* overpotential (Tafel plot, Fig. 2), the data exhibit a linearity over 110 mV and a slope of ~60 mV per decade. This is again analogous to that previously found for a CoPi film,[20] highlighting once more the close resemblance of the present WOC catalyst to CoPi. The above results finally show that electrooxidation of a single monolayer of C/Co-NPs on ITO leads to a very efficient and fast formation of an amorphous film of cobalt-based WOC.

In a next step, we have examined how an increasing deposit of C/Co-NPs onto the electrode as well as how a prolonged anodic bias to the film can influence the formation rate of the catalytic film as well as its efficiency towards water oxidation. Thanks to the intrinsic conductive properties of the nanoparticles, one can expect that the anodic corrosion occurs not only in the first layer of particles in direct electrical contact with the underlying ITO electrode, but also propagates everywhere

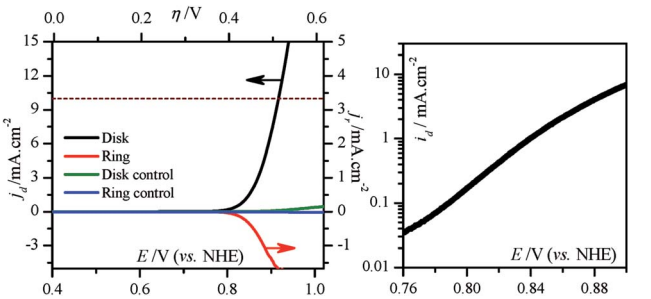


Fig. 2 Left: Linear voltammetric scans ($v = 0.05$ V $s^{-1}$) recorded at a RRDE (rotation rate: 1600 rpm) in 20 mL of 1 M NaOH. For the dark and red plots, the working GC disk electrode of the RRDE was beforehand coated by a Co-based catalytic film (obtained from anodic polarization of a 0.1 mg $cm^{-2}$ C/Co-NPs on GC for 10 min at 1.24 V in 0.1 M NaPi). For the blue and green plots, the working disk electrode is the bare GC disk of the RRDE. The black and green plots are the currents at the GC disk, while the red and blue plots are the currents at the Pt ring biased at a constant potential of −0.46 V. The horizontal dashed line at 10 mA $cm^{-2}$ is the current density expected for a 10% efficient solar water-splitting device. Note that the currents were all normalized to the geometric area of the GC working disk electrode. Right: Tafel plot representation of the black curve on the left graph after it was corrected from the blank response (*i.e.*, subtracted to the green curve on the left graph). $T = 20$ °C.

throughout the conductive porous network of the particulate film. A series of ITO electrodes (E-1 to E-8 in Table 1) coated with different weights of C/Co-NPs (ranging from 0.05 to 5 mg $cm^{-2}$) and activated for different polarization times (ranging from a few seconds to one hour) at a constant anodic potential (1.24 V in 0.1 M NaPi, a potential which is sufficiently high to convert $Co^0$ into $Co^{III}$) were prepared. After activation, the modified electrodes were carefully rinsed with water to remove all particles that had not reacted. The macroscopic and SEM images of electrode surfaces prepared from 3 distinct amounts of C/Co-NPs (E-1, E-2 and E-3), each polarized for 1 h at 1.24 V, are shown in Fig. 3. For comparison, the images of a CoPi-coated electrode prepared by the electrooxidation of a 0.5 mM $Co^{2+}$ solution for 1 h at 1.24 V is also reported (E-4). Macroscopic images clearly show the formation of a film that turns from translucent brown to opaque dark brown when the amount of deposited nanoparticles increases. This indicates that an increasing amount of material is retained on the electrode surface as the thickness of the film covering the electrode is increased, translating into a darker coloration and greater opacity of the film. This also means that under anodic polarization, the particulate film is electrochemically converted into volume, leading to the accretion of the nanoparticles over a definite thickness upright to the ITO surface. When compared to a CoPi film electrodeposited from a 0.5 mM $Co^{2+}$ solution under the same electrodeposition conditions (E-4 in Fig. 3), a much weaker colouration is observed, thereby indicating a much thinner deposit in that case.

The SEM image of the film deposited from the lowest amount of C/Co-NPs showed the characteristic cracks typically observed for a dried homogenous film of amorphous cobalt oxide/hydroxide electrogenerated from a solution of $Co^{2+}$ (compare electrodes E-1 and E-4). Although less easy to discern because masked by an upper layer of aggregated nanoparticles, an underlying homogenous amorphous film with cracks is also present for the higher loads of C/Co-NPs (E-2 and E-3). This is more visible on the cross-sectional view of the film electrodeposited from the highest starting amount of nanoparticles (E-3) for which the thicker (>15 μm) heterogeneous upper layer differs markedly from the thinner (~1 μm) homogeneous lower layer (Fig. S5 and S6†). Whatever the starting amount of C/Co-NPs on ITO, the electrogenerated deposits were finally

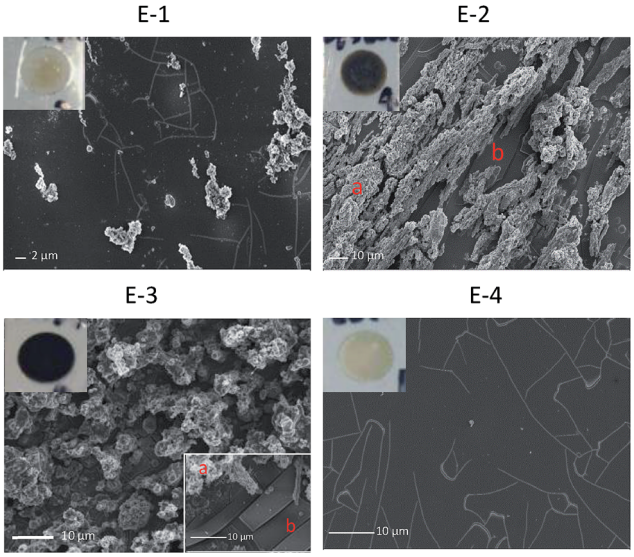


Fig. 3 (E-1 to E-3) SEM and (top left corners) macroscopic images of C/Co-NP-coated ITO electrodes after anodic polarization at 1.24 V for 1 h in 5 mL of 0.1 M NaPi (pH 7.0) followed by rinsing. The initial surface weight of C/Co-NPs on ITO were (E-1) 0.05, (E-2) 0.5, and (E-3) 5 mg $cm^{-2}$. (E-4) SEM and (top left corner) macroscopic image of a CoPi-coated ITO electrode prepared according to Nocera's method (*i.e.*, electrodeposition at 1.24 V for 1 h in a 5 mL solution of 0.5 mM $Co(NO_3)_2$ in 0.1 M NaPi, pH 7.0). Markers a and b on the SEM images designate upper and lower layers, respectively. In E-3, the SEM image added in the bottom right corner allows better visualization of the underlying homogenous layer that is deposited on the ITO electrode surface.

Table 1 Experimental conditions used for the preparation of different CoPi-modified ITO electrodes (during the electrodeposition all electrodes were polarized at 1.24 V *vs.* NHE)

| Electrode number | C/Co-NP amount (mg $cm^{-2}$) | [$Co(NO_3)_2$] (mM) | Electrodep. time (s) | Charge passed (C $cm^{-2}$) |
|---|---|---|---|---|
| E-1 | 0.05 | | 3600 | 1.8 |
| E-2 | 0.5 | | 3600 | 4.4 |
| E-3 | 5 | | 3600 | 6.9 |
| E-4 | | 0.5 | 3600 | 0.6 |
| E-5 | 5 | | 10 | 0.04 |
| E-6 | 5 | | 120 | 0.4 |
| E-7 | 5 | | 600 | 1.4 |
| E-8 | 5 | | 1800 | 3.2 |

consistently made of two distinct layers: (a) a thin homogeneous and uniform underlying layer that cover the entire ITO surface and (b) a thick upper layer of partially corroded and aggregated particles that strongly adhere on the ITO surface. Energy dispersive X-ray analysis (EDX) (Fig. S7 and S8†) showed that both layers contained mainly Co, O and P elements, but with a slightly higher relative content in Co for the upper layer, suggesting the presence of incompletely corroded cobalt nanoparticles in this layer. On the basis of these results, we have concluded that the homogenous underlying layer corresponds to the catalytically active amorphous cobalt hydroxide film which deposits over the ITO surface, while the upper layer corresponds to the nanoparticles that are not completely converted into an amorphous cobalt hydroxide. The presence of these embedded nanoparticles could be advantageous for applications as they could constitute a supply of Co ions for regeneration of the catalytic layer upon additional anodic polarization. From SEM images, it can also be observed a significant change in the morphology of the nanoparticles forming the upper layer, the latter appearing covered and/or entrapped within an amorphous coating. This observation is line with the idea that anodic corrosion occurs over a certain thickness within the conductive particulate film, thus authorizing the deposit of an amorphous cobalt oxide far from the immediate vicinity of the conductive ITO surface. It is however important to note that thicker electrodeposited material does

not necessarily lead to a significant increase in the catalytic activity. This is well-illustrated in Fig. S4† where the magnitude of the catalytic current is only marginally increased with the increase of C/Co-NPs, thus suggesting that only a fraction of the deposited film appreciably takes part in the catalysis of water oxidation under these conditions. It also indicates that the electrochemically generated active film rapidly reaches an optimal value and that excess of nanoparticles is unnecessary. We can thus assume that the fraction that is likely to be the most active for water oxidation is the underlying homogeneous layer, the thickness of which growths rapidly up to an optimal value even when starting from a small amount of cobalt nanoparticles.

To demonstrate that the present methodology is more efficient and faster for the preparation of a cobalt-based WOC film than the previous method based on anodic film deposition from a solution of $Co^{2+}$, we compared the chronoamperometric responses recorded during the anodic polarization of a particulate film of C/Co-NPs on ITO to the one recorded at an anodically polarized bare ITO electrode in a 0.5 mM $Co^{2+}$ solution (Fig. 4). Whatever the electrodeposition mode, the resulting chronoamperometric responses are characteristic of film formations kinetically controlled by a nucleation and growth mechanism, a behaviour that was previously well identified for the electrodeposition of a CoPi film from a solution of $Co^{2+}$.[20] There is however a marked difference in the magnitude of current density which is ~10-fold higher for the film generated from the cobalt particulate film. This result clearly demonstrates a faster film formation when starting from C/Co-NPs instead of soluble $Co^{2+}$.

Other experiments emphasizing the fast and efficient formation of a cobalt-based WOC film from nanoparticles are those reported in Fig. S9† where the catalytic CV response obtained for a very short-time anodic polarization of a cobalt-based particulate film (*i.e.*, 10 s at 1.24 V) is clearly shifted to a more favourable overpotential (~200 mV gain at 5 mA $cm^{-2}$) than a CoPi film electrogenerated from a 0.5 mM $Co^{2+}$ solution during a considerably much longer polarization time (*i.e.*, 1 h at 1.24 V). It remains however important to note that prolonged electrodeposition times do not improve significantly the catalytic performances of the deposited film, these performances reaching rapidly a limiting regime (Fig. 5). This limitation suggests again the formation of an optimal catalytic film thickness where excess of either nanoparticles or electrodeposition times are superfluous. Further studies similar to those previously achieved with films electrodeposited from a $Co^{2+}$ solution[30] are however required to better understand the key parameters governing this limitation. Finally, these results lead us to conclude that a rather small amount of particles is sufficient to produce an optimally active film in a very short time.

In order to determine if the present methodology can be extended to the preparation of other metal-based WOC films, we have investigated the possibility to electrooxidize other metal-based nanoparticulate films. For such a purpose, we have tested commercially available carbon-coated nickel nanoparticles (C/Ni-NPs) synthesized by laser evaporation. We have selected these nanoparticles because their physico-chemical properties and size (~20 nm) were very similar to those of the carbon-coated cobalt nanoparticles, and also because nickel-based amorphous films prepared from electrooxidation of a dilute $Ni^{2+}$ solution were proved effective for producing efficient oxygen-evolving catalysts under benign conditions.[9] We have thus applied the same electrodeposition strategy as for cobalt-based particles by anodically polarizing (600 s at 1.24 V) a particulate film of C/Ni-NPs magnetically collected on an ITO electrode. The NaPi buffer was replaced by a 0.1 M sodium borate buffer (pH 9.2), because the borate anion was previously identified as a preferred coordinating and proton-acceptor in

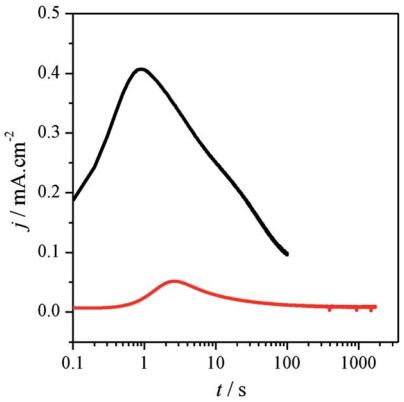


Fig. 4 Chronoamperometric responses recorded at (black) a C/Co-NP-coated ITO electrode (0.05 mg $cm^{-2}$) in 0.1 M NaPi (pH 7.0) and (red) a ITO electrode immersed in a 0.5 mM $Co(NO_3)_2$ solution in 0.1 M NaPi (pH 7.0). The applied potential was in each case of 1.14 V (*vs.* NHE) and the measurements were stopped after an identical amount of charge has been passed (*i.e.*, 16 mC $cm^{-2}$).

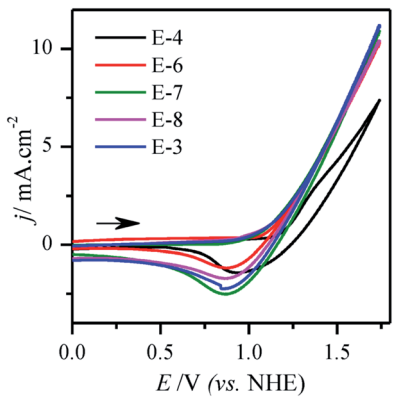


Fig. 5 CVs ($v$ = 0.1 V $s^{-1}$) of C/Co-NP-coated ITO electrodes (5 mg $cm^{-2}$) that were beforehand submitted to an anodic polarization (1.24 V) in 0.1 M NaPi for a period of (E-6, red) 120, (E-7, green) 600, (E-8, blue) 1800, and (E-3, cyan) 3600 s, followed by rinsing and CV characterization in a fresh buffer solution of 0.1 M NaPi (pH 7.0). For comparison, (E-4, black) the CV ($v$ = 0.1 V $s^{-1}$) of a CoPi-coated ITO electrode is shown. In this case, the CoPi deposit was obtained from anodic electrodeposition at 1.24 V for 1 h in a 0.5 mM solution of $Co^{2+}$, and the resulting rinsed CoPi-coated ITO electrode was characterized by CV in 0.1 M NaPi (pH 7.0). All experiments were carried out at room temperature.

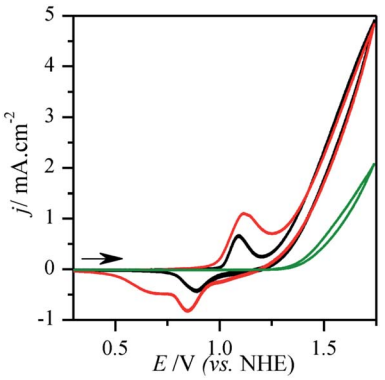


Fig. 6 CVs ($v = 0.1$ V s$^{-1}$) of C/Ni-NP-coated ITO electrodes that were beforehand polarized for 600 s at 1.24 V in a 0.1 M borate buffer (pH 9.2), followed by rinsing and characterization by CV in a fresh solution of 0.1 M borate buffer (pH 9.2). The initial amount of C/Ni-NPs collected on the electrode surface was (black) 0.05 mg cm$^{-2}$ and (red) 0.5 mg cm$^{-2}$. As a control, the CV of a bare ITO electrode having been subjected to the same treatment but without nanoparticles is shown in green. All experiments were carried out at room temperature.

the formation of a catalytic film.[9] After electrode rinsing, the resulting modified electrode was scanned by CV in a fresh solution of borate buffer (Fig. 6). As expected and similar to what was previously described for an amorphous nickel oxide/hydroxide film, the CV shows a sharp anodic surface wave centred at 1.1 V assigned to the oxidation of a surface adsorbed $Ni^{II}$ oxide/hydroxide species followed by an exponential catalytic current increase with an onset potential of 1.25 V characteristic of the catalytic oxidation of water, while during the cathodic return scan the CV shows a broad feature at 0.85 V corresponding to the reduction of the previously oxidized surface adsorbed nickel oxide/hydroxide species. Moreover, as shown in Fig. 6, the anodic and cathodic prefeatures increase in amplitude when increasing the starting amount of magnetically collected nanoparticles, suggesting a growth in the surface electrodeposited material. Finally, similar to what was previously shown from dilute $Ni^{2+}$ solution,[9] neither film formation nor catalysis was observed in the absence of the borate electrolyte, thus attesting to the strong similarity between the nickel-based WOCs obtained from electrooxidation of a $Ni^{2+}$ solution in a borate buffer and the one resulting from anodic corrosion/dissolution of a particulate film of C/Ni-NPs.

## Conclusions

Metal-based nanoparticles magnetically collected on an electrode surface are effective substrates for the electrodeposition of amorphous metal-based oxide/hydroxide water oxidation catalysts on an electrode surface. The new methodology proposed here is significant because it offers the possibility to produce, under mild conditions and in a very short time, a relatively thick and highly efficient catalytic film for water oxidation at neutral pH. Compared to amorphous films formed by anodic electrodeposition of a metal salt in solution, a key advantage of the proposed approach is supplying the metal ion in a solid and metallic form. This plays a decisive role in the catalytic film formation rate, leading to the deposition of the oxygen-evolving catalyst in a remarkably short-time. In addition, given the magnetic properties of the particles, this metal solid phase can be easily manipulated under a magnetic field to form a precursor particulate film, a process that is fast and easy to implement. It also provides the opportunity to recover and reuse the excess of cobalt nanoparticles, not only immediately after the electrodeposition of the catalytic film, but also for film regeneration when necessary. This may be advantageous for an industrial process for both reducing the costs and better handling the risk of environmental contamination by heavy metal ions. Finally, the new electrodeposition strategy we proposed can be easily extended to a wide range of metal particles of different nature and sizes, and also their mixture, thus offering a new degree of flexibility and opportunities not only in the preparation of metal-based water oxidation catalysts, but also in the preparation of inorganic metal-based catalysts for hydrogen[31] or oxygen evolution.[32]

## Acknowledgements

We are very grateful to Helene Lecocq for the SEM images and to Jean-Yves Piquemal for XRD analysis. We want to acknowledge the GENS-ECNU program and the China Scholarship Council for J. Zhu PhD fellowship.

## Notes and references

1 T. R. Cook, D. K. Dogutan, S. Y. Reece, Y. Surendranath, T. S. Teets and D. G. Nocera, *Chem. Rev.*, 2010, **110**, 6474–6502.
2 J. R. McKone, N. S. Lewis and H. B. Gray, *Chem. Mater.*, 2013, **26**, 407–414.
3 V. Artero, M. Chavarot-Kerlidou and M. Fontecave, *Angew. Chem., Int. Ed.*, 2011, **50**, 7238–7266.
4 B. A. Pinaud, J. D. Benck, L. C. Seitz, A. J. Forman, Z. Chen, T. G. Deutsch, B. D. James, K. N. Baum, G. N. Baum, S. Ardo, H. Wang, E. Miller and T. F. Jaramillo, *Energy Environ. Sci.*, 2013, **6**, 1983–2002.
5 D. G. Nocera, *Inorg. Chem.*, 2009, **48**, 10001–10017.
6 X. Deng and H. Tüysüz, *ACS Catal.*, 2014, **4**, 3701–3714.
7 C. C. L. McCrory, S. Jung, J. C. Peters and T. F. Jaramillo, *J. Am. Chem. Soc.*, 2013, **135**, 16977–16987.
8 M. W. Kanan and D. G. Nocera, *Science*, 2008, **321**, 1072–1075.
9 M. Dincă, Y. Surendranath and D. G. Nocera, *Proc. Natl. Acad. Sci. U. S. A.*, 2010, **107**, 10337–10341.
10 M. Gao, W. Sheng, Z. Zhuang, Q. Fang, S. Gu, J. Jiang and Y. Yan, *J. Am. Chem. Soc.*, 2014, **136**, 7077–7084.
11 W. D. Chemelewski, H.-C. Lee, J.-F. Lin, A. J. Bard and C. B. Mullins, *J. Am. Chem. Soc.*, 2014, **136**, 2843–2850.
12 I. Zaharieva, P. Chernev, M. Risch, K. Klingan, M. Kohlhoff, A. Fischer and H. Dau, *Energy Environ. Sci.*, 2012, **5**, 7081–7089.
13 E. R. Young, D. G. Nocera and V. Bulovic, *Energy Environ. Sci.*, 2010, **3**, 1726–1728.

 

14 M. J. Kenney, M. Gong, Y. Li, J. Z. Wu, J. Feng, M. Lanza and H. Dai, *Science*, 2013, **342**, 836–840.
15 R. D. L. Smith, M. S. Prévot, R. D. Fagan, Z. Zhang, P. A. Sedach, M. K. J. Siu, S. Trudel and C. P. Berlinguette, *Science*, 2013, **340**, 60–63.
16 R. D. L. Smith, M. S. Prévot, R. D. Fagan, S. Trudel and C. P. Berlinguette, *J. Am. Chem. Soc.*, 2013, **135**, 11580–11586.
17 R. N. Grass, E. K. Athanassiou and W. J. Stark, *Angew. Chem., Int. Ed.*, 2007, **46**, 4909–4912.
18 Y. Surendranath, M. Dincă and D. G. Nocera, *J. Am. Chem. Soc.*, 2009, **131**, 2615–2620.
19 This is the further oxidation of the $Co^{III}$-based film that is assumed to produce a $Co^{IV}$ species able to oxidize water into $O_2$, thereby leading to a back regeneration of the $Co^{II}$ species for a new catalytic round.
20 Y. Surendranath, D. A. Lutterman, Y. Liu and D. G. Nocera, *J. Am. Chem. Soc.*, 2012, **134**, 6326–6336.
21 Analytical Chemistry – Electrochemical Series, in *CRC Handbook of Chemistry and Physics*, Internet Version, ed. D. R. Lide, CRC Press/Taylor and Francis, Boca Raton, FL, 90th edn, 2010.
22 A. J. Esswein, M. J. McMurdo, P. N. Ross, A. T. Bell and T. D. Tilley, *J. Phys. Chem. C*, 2009, **113**, 15068–15072.
23 R. N. Singh, D. Mishra, A. S. K. Anindita Sinha and A. Singh, *Electrochem. Commun.*, 2007, **9**, 1369–1373.
24 C. Iwakura, A. Honji and H. Tamura, *Electrochim. Acta*, 1981, **26**, 1319–1326.
25 T. Schmidt and H. Wendt, *Electrochim. Acta*, 1994, **39**, 1763–1767.
26 F. Jiao and H. Frei, *Angew. Chem., Int. Ed.*, 2009, **48**, 1841–1844.
27 A. Harriman, I. J. Pickering, J. M. Thomas and P. A. J. Christensen, *J. Chem. Soc., Faraday Trans. 1*, 1988, **84**, 2795–2806.
28 The RRDE experiment has been performed in 1 M NaOH for the reason that at this pH the reduction $O_2$ to $H_2O_2$ is much better defined than at neutral pH.
29 M. G. Walter, E. L. Warren, J. R. McKone, S. W. Boettcher, Q. Mi, E. A. Santori and N. S. Lewis, *Chem. Rev.*, 2010, **110**, 6446–6473.
30 D. K. Bediako, C. Costentin, E. C. Jones, D. G. Nocera and J.-M. Savéant, *J. Am. Chem. Soc.*, 2013, **135**, 10492–10502.
31 S. Cobo, J. Heidkamp, P.-A. Jacques, J. Fize, V. Fourmond, L. Guetaz, B. Jousselme, V. Ivanova, H. Dau, S. Palacin, M. Fontecave and V. Artero, *Nat. Mater.*, 2012, **11**, 802–807.
32 A. Indra, P. W. Menezes, N. R. Sahraie, A. Bergmann, C. Das, M. Tallarida, D. Schmeiβer, P. Strasser and M. Driess, *J. Am. Chem. Soc.*, 2014, **136**, 17530–17536.